

ScienceDirect

FAC Papers Online

IFAC PapersOnLine 55-37 (2022) 764-769

Stabilization of an Inverted Pendulum on a Nonholonomic System

Kartik Loya * Phanindra Tallapragada *

* Department of Mechanical Engineering, Clemson University, SC, 29634, USA (e-mail: ptallap@clemson.edu)

Abstract: In this paper we investigate the problem of stabilizing the roll dynamics of a nonholonomic system that is inspired by a Chaplygin sleigh whose center of mass is at some height above the ground. The sole actuation for the extruded Chaplygin sleigh, is via the motion of an internal reaction wheel which applies a torque in the yaw direction. This torque is used to propel the Chaplygin sleigh as well as stabilize its roll. This system is motivated by the problem of the stabilization of the roll of a fish-like underwater swimmer. The dynamics of a fish-like swimmer have been shown to be similar to that of a Chaplygin sleigh. We propose a feedback control, by considering the associated linear representation due to the action of a Koopman operator on the observables. Using the Koopman operator, a constrained optimal control problem is formulated in the lifted space which we solve using model predictive control. The approach has the advantage of being systematically generalized for increased model complexity for nonholonomic systems and actuator saturation.

Copyright © 2022 The Authors. This is an open access article under the CC BY-NC-ND license (https://creativecommons.org/licenses/by-nc-nd/4.0/)

Keywords: Non-holonomic system, inverted-pendulum Stabilization, Koopman MPC

1. INTRODUCTION

In this paper we investigate the problem of stabilizing the roll dynamics of a nonholonomic system that is inspired by a Chaplygin sleigh see (Bloch, 2003), (Borisov and Mamaev, 2003; Borisov et al., 2007) and (Neimark and Fufaev, 1972) for a review. The Chaplygin sleigh is a planar system, with configuration manifold SE(2) and a single nonholonomic constraint on its velocity. We consider a modified Chaplygin sleigh whose center of mass is not at ground height, with a configuration manifold $S^1 \times$ SE(2). Such a rigid body has a tendency to "fall down" since the upward position of the center of mass is an unstable equilibrium. The only actuator for the system under consideration is an internal reaction wheel. The motion of the reaction wheel produces a torque on the Chaplygin sleigh that can propel it with side-to-side sway and yaw motion and is intended to simultaneously stabilize the roll motion of the sleigh.

The modified Chaplygin sleigh with roll dynamics is inspired by recent research on underwater fish-like swimmers. The dynamics of such swimmers, in the approximation of in-viscid flow, have been shown to possess a nonholonomic constraint similar to that of the Chaplygin sleigh in (Tallapragada, 2015) and (Tallapragada and Kelly, 2016) and has found application in the design and control of underwater robots (Pollard and Tallapragada, 2017; Free et al., 2020). The simplified dynamics of such swimmers are entirely planar and do not consider the effects of unstable roll motion; the geometric shapes of such robots are such that roll motion is negligible due

to the buoyancy force. This comes at the cost of agility and efficiency while highly efficient and agile biological swimmers tend to be roll unstable (Webb and Weihs, 2015).

The problem investigated in this paper adds to the well studied class of problems related to the stabilizing of a unicycle's dynamics. The stability of the unicycle and its variations has been investigated using geometric methods, see for example (Zenkov et al., 1999) and (Bloch et al., 1997), feedback linearization of the kinematic unicycle in (De Luca et al., 2000) and sliding mode control for example by (Thomas et al., 2019). The work in this paper is distinct from such research in a few key aspects. The dynamics of the Chaplygin sleigh with roll motion are different from that of the unicycle. The spin angular momentum of a unicycle has a stabilizing effect on its roll motion, at fast spin speeds a unicycle with a rider is easily stabilized as shown in (Zenkov et al., 1999) and (Zenkov et al., 2002). The Chaplygin sleigh has no such spin angular momentum.

The proposed approach in this paper uses the linear dynamics on a lifted space via the Koopman operator. Using the Koopman operator, a constrained optimal control problem is formulated in this lifted space which we solve using model predictive control. This approach is inspired by recent progress on Koopman operator methods to control systems, see for example (Korda and Mezic, 2018; Ma et al., 2019) and particularly for robotics see for example (Abraham et al., 2017; Y. Han and Vaidya, 2020; Otto and Rowley, 2021). In particular (Korda and Mezic, 2018) proposes an approach to formulate a high dimensional linear control system that is amenable to model predictive control (MPC).

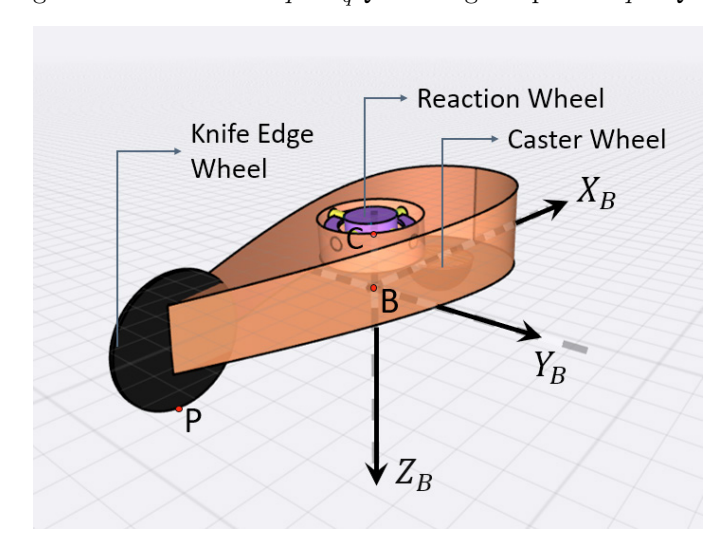
 $[\]star$ This work was supported by grant 2021612 from the National Science Foundation and grant 13204704 from the Office of Naval Research.

The physical system investigated in this paper, a Chaplygin sleigh with roll dynamics, as well as the application of the control approach using the lifted dynamics via the Koopman operator to stabilization problems in nonholonomic systems are novel. The physical system modeling can be extended to high degree of freedom nonholonomic ground systems as well as to fish-like swimming robots. More importantly the control approach is amenable to incorporate further constraints like actuator saturation, to increasing model complexity seen in a realistic robot and to achieve other goals like simultaneous path tracking.

2. SYSTEM MODELING

2.1 Kinematics

The Chaplygin sleigh or cart, shown in Fig. 1, has a knife edge or a small inertia-less wheel at the rear at point P and is supported on a single caster wheel at the front that allows motion in any direction. The sleigh is also assumed to have an internal reaction wheel, whose angular acceleration can transfer a torque on the sleigh. The configuration manifold of the physical system is $Q = SE(2) \times S^1$ parameterized locally by $q = (x_c, y_c, \theta, \psi)$, with generalized velocities $\dot{q} \in T_q Q$ the tangent space to $q \in Q$.



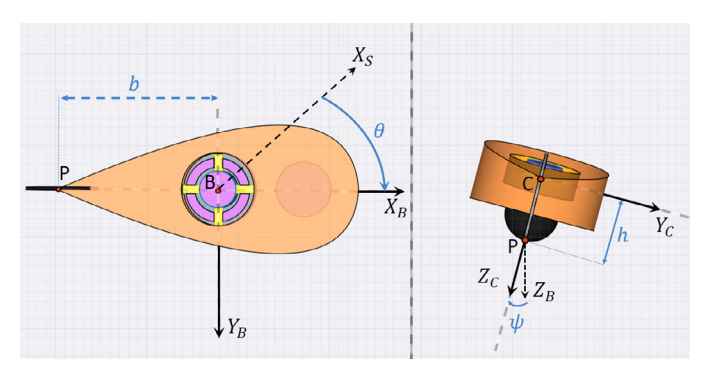


Fig. 1. Geometric model for the Chaplygin sleigh with rolling dynamics. Top and back view showing yawing and rolling motion respectively.

Here we do not include a generalized coordinate associated with the internal reaction wheel, but instead include the torque generated by it is as a control input in the latter equations of motion. The spatial frame is denoted by \mathcal{F}_S with axes $X_s - Y_s - Z_s$. The center of mass of the sleigh is at point C with coordinates $(x_c, y_c, -h)$ in the spatial frame (X_s, Y_s, Z_s) and point B is its projection on the ground with coordinates $(x_c, y_c, 0)$. Additionally the body frame collocated at B and rotated by the yaw angle θ with respect to the spatial frame is denoted by \mathcal{F}_B with axes $X_b - Y_b - Z_b$; body frame attached at point C and rotated by the yaw angle ψ with respect to the frame B is denoted by \mathcal{F}_c with axes $X_c - Y_c - Z_c$. The coordinates of P in frame \mathcal{F}_b are (-b, 0, 0). The angular velocity of the frame \mathcal{F}_b with respect to the spatial frame is

$$[\omega_B] = \begin{bmatrix} \dot{\psi} \\ \dot{\theta} \sin \psi \\ \dot{\theta} \cos \psi \end{bmatrix} \tag{1}$$

The velocity (\dot{x}_c, \dot{y}_c) in the spatial frame transform to (u, v) in the \mathcal{F}_B frame as

$$[u\ v]^{\mathsf{T}} = R_{sb} \cdot [\dot{x}_c\ \dot{y}_c]^{\mathsf{T}} \tag{2}$$

With this notation the velocity of the center of mass C in frame \mathcal{F}_c is

$$V_C^c = \begin{bmatrix} u - h\dot{\theta}\sin\psi\\ v + h\dot{\psi}\cos\psi\\ h\dot{\psi}\sin\psi \end{bmatrix}$$
 (3)

We assume that the rear wheel at P prevents slipping in the transverse (X_b) direction but rolls without any slipping in the longitudinal direction along (Y_b) . While $dim(T_qQ)=4$, the nonholonomic constraint at point P given by

$$\begin{split} V_P^B = [-\sin\theta \; \cos\theta \; -b \; \; 0] [\dot{x} \; \; \dot{y} \; \; \dot{\theta} \; \dot{\psi} \; \; 0]^\intercal = 0 \\ & \quad \text{or} \quad v - b\dot{\theta} = 0 \end{split} \tag{4}$$

restricts the velocity $\dot{q} \in W(q) \subset T_qQ$, where dim(W(q)) = 3. Therefore a reduced set of velocities $(u, \dot{\theta}, \dot{\psi})$ span the space W(q) of allowable velocities.

2.2 Equations of motions

Suppose the mass of the Chaplygin sleigh is m, its moment of inertia tensor is I_B , the Lagrangian for the Chaplygin sleigh is $\mathcal{L} = \mathcal{T} - \mathcal{V}$ where

$$\mathcal{T} = \frac{1}{2} \Big(V_C^c \cdot M \cdot V_C^c + \omega_B^{\mathsf{T}} \cdot I_B \cdot \omega_B \Big)$$

is the kinetic energy with M as a 3×3 diagonal mass tensor with diagonal entries being m and potential energy is $\mathcal{V} = mgh \cdot \cos \psi$. We also assume viscous dissipation of energy with Raleigh dissipation function

$$\mathcal{R}(u,\dot{\theta},\dot{\psi}) = \frac{1}{2}(C_u u^2 + C_{\psi}\dot{\psi}^2 + C_{\theta}\dot{\theta}^2)$$

defined in terms of the reduced velocities $(u, \dot{\theta}, \dot{\psi})$. The same dissipation function can also be written in the spatial velocities by transforming the velocity $[u, v] = R_{sb}^{\mathsf{T}}[u \quad 0]^{\mathsf{T}}$ and using the nonholonomic constraint $v = b\dot{\theta}$ giving $\mathcal{R}(\dot{x}_c, \dot{y}_c, \dot{\theta}, \dot{\psi}) = \mathcal{R}(R_{sb}^{\mathsf{T}}[u \quad 0]^{\mathsf{T}}, \dot{\theta}, \dot{\psi})$.

The Euler Lagrange equations for the Chaplygin sleigh are then

$$\frac{\mathrm{d}}{\mathrm{d}t} \left(\frac{\partial}{\partial \dot{q}^k} \mathcal{L} \right) - \frac{\partial \mathcal{L}}{\partial q^k} = C_{jk} \lambda_k + Q_k + \Gamma$$

Where, $Q_k = \frac{\partial}{\partial \dot{q}^k} \mathcal{R}(\dot{x}_c, \dot{y}_c, \dot{\theta}, \dot{\psi})$ is the force due to viscous dissipation along longitudinal velocity and damping in the

yaw and roll motion. The Lagrange multiplier λ_k are the constraint forces and C_{jk} are the coefficients of the pfaffian one form, with kth row $C_k = [-\sin\theta \quad \cos\theta \quad -b \quad 0]$ and τ is the torque generated by the reaction wheel in the yaw direction. Straight forward calculations yield the equations of motion as

$$\mathcal{M}(\psi)\dot{\xi} + \mathcal{C}(\psi,\dot{\psi},\dot{\theta})\xi + \mathcal{G}(\psi) = \Gamma \tag{5}$$

where \mathcal{M} is the mass matrix, \mathcal{C} the centrifugal terms, \mathcal{G} are the gravitational terms with $\xi = [u, \dot{\theta}, \dot{\psi}, \psi]$ and

$$\mathcal{M}_{11} = -m , \ \mathcal{M}_{33} = -(I_{Cx} + mh^2) , \ \mathcal{M}_{44} = 1$$

$$\mathcal{M}_{22} = -\left(m(h^2 \sin^2(\psi) + b^2) + I_{cy} \sin^2(\psi) + I_{cz} \cos^2(\psi)\right)$$

$$\mathcal{M}_{12} = \mathcal{M}_{21} = mh \sin \psi , \ \mathcal{M}_{23} = \mathcal{M}_{32} = mh \sin(\psi)$$

$$\begin{aligned} &\mathcal{C}_{11} = -C_u \;, & \mathcal{C}_{12} = m(b\dot{\theta} + 2h\dot{\psi}\cos\psi) \\ &\mathcal{C}_{33} = -C_{\psi} \;, & \mathcal{C}_{31} = -mh\dot{\theta}\cos\psi \;\;, & \mathcal{C}_{23} = mbh\dot{\psi}\sin(\psi) \\ &\mathcal{C}_{43} = 1 \;, & \mathcal{C}_{22} = -C_{\theta}\dot{\theta} - \dot{\psi}\sin(2\psi)(mh^2 + I_{cy} - I_{cz}) \\ &\mathcal{C}_{21} = -mb\dot{\theta} \;, & \mathcal{C}_{32} = \frac{(\dot{\theta}\sin(2\psi)(mh^2 + I_{cy} - I_{cz}))}{2} \\ &\Gamma = [0 \;\; \tau \; 0 \;\; 0]^{\mathsf{T}} \;\;, & \mathcal{G} = [0 \;\; 0 \;\; -mg\cos(\psi) \;\; 0]^{\mathsf{T}} \end{aligned}$$

The matrix terms not mentioned are 0. The dynamical system (5) is four dimensional, with states ξ being only the reduced velocity and the internal shape variable ψ . The equations of motion of the Chaplygin are SE2 invariant enabling the decoupling of the reduced velocity equations from equations governing the evolution of (x, y, θ) . The solution $(x(t), y(t), \theta(t))$ can be obtained by integrating (2).

3. KOOPMAN LIFTING AND MPC FORMULATION

The control problems with non-linear dynamics have been extensively studied and there are abundant modern optimal control techniques with numerical optimization tools like modern predictive control, feedback linearization and sliding mode control etc. These various nonlinear control techniques help in computing satisfactory solutions for nonlinear and high fidelity systems but the challenge here is to implement these techniques in real time and with accuracy in uncertain environment which is important for robotic systems. Therefore to overcome this balance of high computational cost and model accuracy, approximate linear models representing the nonlinear systems are used. The models created through local linearization around a trajectory or fixed point are valid only locally which may result in sub-optimal or even inaccurate solutions due to deviations from the local region. To address these challenges a linear predictor is needed which encapsulates the non-linearity of the system for better accuracy. One such linear predictor is the Koopman operator which transforms or lifts a nonlinear system into a higher dimensional linear system on which linear control methodologies can be applied.

3.1 Linear predictor (Koopman Operator)

While the control system in (5) is continuous in time, we consider a discrete time system in the formulation for the control problem. Consider a discrete time dimensional dynamical system

$$x_{t+1} = F(x_t) \tag{6}$$

with states $x \in \mathbb{X} \subset \mathbb{R}^n$. The map $F: \mathbb{R}^n \times \mathbb{R}^m \to \mathbb{R}^n$ is equivalent to the flow map of a continuous time control system advances for a chosen time step. The Koopman operator is an infinite dimensional linear operator which propagates observable functions of the states forward in time under the dynamics of the system. The action of the Koopman operator $\mathcal{K}: \mathcal{L}^\infty(\mathbb{X}) \mapsto \mathcal{L}^\infty(\mathbb{X})$ on an observable function $g: \mathbb{X} \mapsto \mathbb{X}$ is given as follows

$$\mathcal{K}g(x_t) = (g \circ F)(x_t) = g(x_{t+1}) \tag{7}$$

see (Lasota and Mackey, 1994) or (Budisic et al., 2012) for a review of the Koopman operator in dynamical systems. To approximate the infinite dimensional operator \mathcal{K} , we take the approach of extended dynamic mode decomposition (EDMD), as proposed in Williams et al. (2015), by projecting the observable function g onto the space spanned by a set, \mathbb{D} , of dictionary functions,

$$\mathbb{D} = \{\psi_1, \psi_2, \dots, \psi_k\} \tag{8}$$

That is, we make the approximation

$$\mathcal{K}g(x_t) \approx \mathcal{K}(c\Psi^{\mathsf{T}})(x_t) \approx c^{\mathsf{T}}K^{\mathsf{T}}\Psi(x_t)$$
 (9)

where $\Psi: \mathbb{X} \to \mathbb{R}^k$ is a column-vector valued function where the elements are given by $[\Psi(x)]_i = \psi_i(x)$, $c \in \mathbb{R}^k$ is a column vector of coefficients, and $K \in \mathbb{R}^{k \times k}$ is the projection of Koopman operator onto the space of functions spanned by the dictionary \mathbb{D} .

To compute the matrix approximation K of the Koopman operator from data, we gather and store data in the form of snapshot matrices

$$X = [x_1 , \cdots, x_m] \tag{10}$$

$$Y = [y_1, \dots, y_m] \tag{11}$$

where the matrices X and Y contain m state observations on the columns. Here we assume that the observables are the states themselves, i.e. y=g(x). We then lift the measurement data by evaluating the dictionary functions at each measurement to obtain the lifted data matrices $\Psi_X, \Psi_Y \in \mathbb{R}^{k \times m}$ as follows.

$$\Psi_X = [\Psi(x_1) , \cdots , \Psi(x_m)] \tag{12}$$

$$\Psi_Y = [\Psi(y_1) , \cdots , \Psi(y_m)] \tag{13}$$

Then, following from Eqs. (7) and (9), we have

$$\Psi_Y = K^{\mathsf{T}} \Psi_X \tag{14}$$

With this, K can be approximately computed by the following least-squares minimization

$$\min_{K} \|\Psi_Y \Psi_X^{\mathsf{T}} - K^{\mathsf{T}} \Psi_X \Psi_X^{\mathsf{T}} \|_2^2 \tag{15}$$

where the least squares problem has been written in normal form so that the minimization only depends on the number of dictionary functions used in the projection, not on the number of measurements.

3.2 Controlled systems

For a control system of the form

$$x_{t+1} = F_u(x_t, \tau_t) \tag{16}$$

where $\tau_t \in \mathbb{U} \subset \mathbb{R}^p$ is the control input and $F_u : \mathbb{X} \times \mathbb{U} \mapsto \mathbb{X}$, we take a similar approach to obtain a linear

representation of the system in a lifted space. That is, we seek a linear approximation of the form

$$\Psi(x_{t+1}) = A\Psi(x_t) + B\tau_t \tag{17}$$

where $A \in \mathbb{R}^{k \times k}$ and $B \in \mathbb{R}^{k \times p}$ are linear predictors computed from observed trajectory data. To obtain such an approximation from data, we gather data in the form of snapshot matrices

$$X = [x_1 , \cdots, x_m] \tag{18}$$

$$Y = [y_1 , \cdots, y_m] \tag{19}$$

$$\Gamma = [\tau_1 \ , \ \cdots \ , \ \tau_m] \tag{20}$$

as before, where we now have m state observations with $y_i = F_u(x_i, u_i)$ for i = 1, ..., m. We then lift the X and Y data as in Eqs. (12) and (13) and perform the minimization

$$\min_{A,B} \|\Psi_Y - A\Psi_X - B\Gamma\|_2^2 \tag{21}$$

or as a least squares problem,

$$\min_{M} \|V - MW\|_{2}^{2} \tag{22}$$

where

$$W = \begin{bmatrix} \Psi_X \\ \Gamma \end{bmatrix} \begin{bmatrix} \Psi_X \\ \Gamma \end{bmatrix}^{\mathsf{T}} \ , \ V = \Psi_Y \begin{bmatrix} \Psi_X \\ \Gamma \end{bmatrix}^{\mathsf{T}} \ , \ M = [A \ B]$$

A is given by the first k columns of M, and B is given by the final p columns of $M \in \mathbb{R}^{k \times (k+p)}$.

The lifted states are brought back to the lower dimensional original states using the matrix C which is calculated again by solving a least square minimization

$$\min_{C} \|X - C\Psi_X\|_2^2 \tag{23}$$

3.3 Koopman Operator for Chaplygin Sleigh

The control-affine nonlinear system (5) can be represented in discrete time

$$\xi_{t+1} = f_d(\xi_t) + f_c(\tau_t) \tag{24}$$

with $\xi_t = [u_t, \dot{\theta}_t, \dot{\psi}_t, \psi_t] \in \mathbb{R}^4$ and the control input torque (τ_t) being the time discretized torque; with p = 1. The lifted functions (Ψ) chosen in this paper are monomial functions of the four states $\xi = [u, \dot{\theta}, \psi, \dot{\psi}]$ upto degree of 4. These basis functions exclude the yaw angle, θ or the position of the sleigh in the plane (x_c, y_c) as equations of motion (5) are SE2 invariant. The lifted functions are

$$\Psi_i(\xi) = u^{i_1} \cdot \dot{\theta}^{i_2} \cdot \psi^{i_3} \cdot \dot{\psi}^{i_4} \tag{25}$$

where (i_1, i_2, i_3, i_4) are positive integers and $0 \leq [i_1 + i_2]$ $i_2 + i_3 + i_4 \le 4$ which creates $N_l = 70$ basis vectors for the lifted space. We then create the learning data set by discretizing the full nonlinear system (5) into nonlinear discrete system (24) using a fourth order Runge-Kutta method and time step $\delta t = 0.001$. The learning data set was collected by selecting random N_{tr} initial conditions of the four states. Then simulated the discrete system for N_{tr} initial conditions over N_k time-step and hence collected $m = N_{tr} \times N_k$ data points. This gives us the required snapshot matrix X, and Y of size $(n \times N_{tr})$ (N_k+1)). The control input (τ) for the simulation was generated randomly with uniform distribution over the interval [-75, 75]Nm and has a size of $(p \times N_{tr} \cdot N_k)$. The uniformly distributed random initial conditions selected for longitudinal velocity (u) in the range [0, 20]m/s and for yaw rate $(\dot{\theta})$ it is [-40, 40] rad/s. For the roll (ψ)

the range is $[-2\pi, 2\pi]$ and the range for roll rate (ψ) is [-20, 20]rad/s. The random initial condition for roll and roll rate is collected in Gaussian distribution with zero mean. These collected snapshot data is lifted to higher dimensional by vector-valued functions (Ψ) and then used to obtain matrices A, B and C through least square minimization shown above (22) or analytical solution given in (Korda and Mezic, 2018). The Koopman operator (K)is approximated by A and B which acts as one step linear predictor for the system (24). In our case the lifting functions contain the states itself and therefore Ψ can be re-arranged to obtain $C=[I_{n\times n}\ 0_{n\times (k-n)}]$. The Koopman operator is constructed with $N_{tr}=200$ and $N_k=1000$ is compared with the nonlinear system for its response to control inputs arbitrarily given to generate a trajectory. The goal here is to see if our Koopman operator is a good linear predictor of the nonlinear Chaplygin sleigh with rolling dynamics (5), which is simulated through numerical integration using fourth order Runge-Kutta method or ode45. The constant parameters of the system (5) selected for simulation are mass $(m = 2.5 \text{ kg}), [C_u, C_\theta, C_\psi] =$ [0.85, 0.85, 0.9], height of center of mass h = 5 cm and co-ordinate of point P is b = 15 cm. The Fig.(2) shows Koopman linear system prediction in dotted red trajectory and the blue trajectory are the solutions of integration of the whole nonlinear system using numerical integration method such as ode45.

3.4 MPC Formulation

The identified linear Koopman operator now can be used to control the nonlinear system with linear control techniques, here we use linear Model predictive Control method. MPC is a multi variable control algorithm which consist of a cost function, a dynamic model, state-input constraints and an optimizer that minimizes the cost function for a specific sample time on a receding horizon. The MPC iterates the process of optimization by first sampling the states for the current time step (t_i) and then for N_p (prediction horizon) time steps it computes a cost minimizing control strategy that predicts future states and control inputs while satisfying constraints. A part of the predicted solution is implemented for N_c (control horizon) time step. Then again the system states are updated and the process continues. MPC for the linear Koopman system obtained in previous section is given as a quadratic optimization problem.

$$\min_{\Psi, \ \tau} \sum_{j=t_i}^{t_i + N_p} \frac{1}{2} \Big(\Psi^{\intercal} \cdot Q_j \cdot \Psi + \tau^{\intercal} \cdot R_j \cdot \tau_j \Big)$$

subject to

$$\Psi_{j+1} = A \ \Psi_j + B \ \tau_j, \qquad j = t_i.... N_p$$

$$\xi_j = C \ \Psi_j$$

$$\tau_{min} \le \tau_j \le \tau_{max}$$

Where, Q and R are positive semidefinite weight matrices, t_i is the initial time and N_p is the prediction horizon. Our goal is to design a Model predictive controller (MPC) that stabilizes the statically unstable roll motion of the modified chaplygin sleigh. We select a diagonal Q matrix with weights that activates cost on divergence of state variable ψ from the reference 0° and also minimizing the

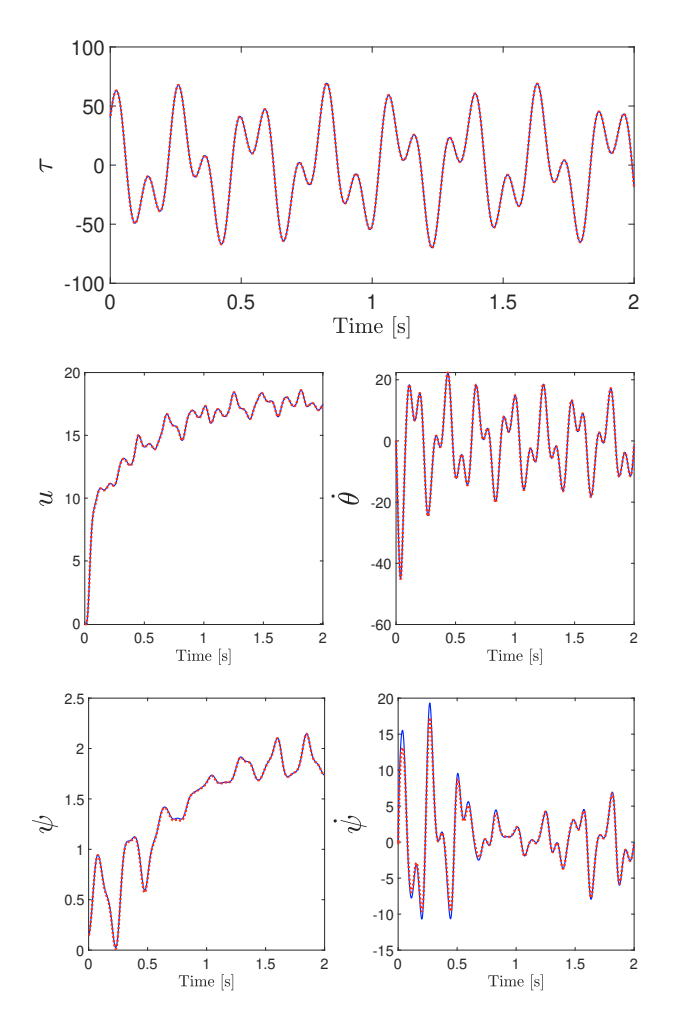


Fig. 2. The figure compares the prediction of the constructed Koopman operator at each time-step with that of nonlinear system simulated through numerical integration using ODE45. The initial condition for the states is $[u, \dot{\theta}, \psi, \dot{\psi}] = [0, 0.1, 0.15, 0]$. The input torque is the periodic function of time $\tau = 20 \cdot \sin(30t) + 25 \cdot \cos(20t)$

control action with weight matrix R. The cost function then becomes

$$J = \sum_{i=t_i}^{t_i + N_p} q_{\psi,j} \cdot \psi_j^2 + r_j \cdot \tau_j^2$$

here, $q_{\psi,j}$ is the diagonal element of the Q_j matrix that activates the cost on deviation of roll angle and r_j is the diagonal element of the R matrix that activates the cost on the control action.

4. RESULTS

Let $N_p=0.01$ and $N_c=0.001$, the initial states are $[u,\ \dot{\theta},\ \psi,\ \dot{\psi}]=[2,\ 0,\ 0.35,\ 0.15]$ and the maximum torque available is $\pm 50\ Nm$. In these results the Koopman MPC after every 10 time steps updates the system states through feedback from the true system that is in this case through the numerical integration of equations of motions. The control torque obtained through this method is applied to the true system. The Fig.(3) shows the unstable nonlinear system with small perturbation can be

stabilized using the control obtained through Koopman MPC.

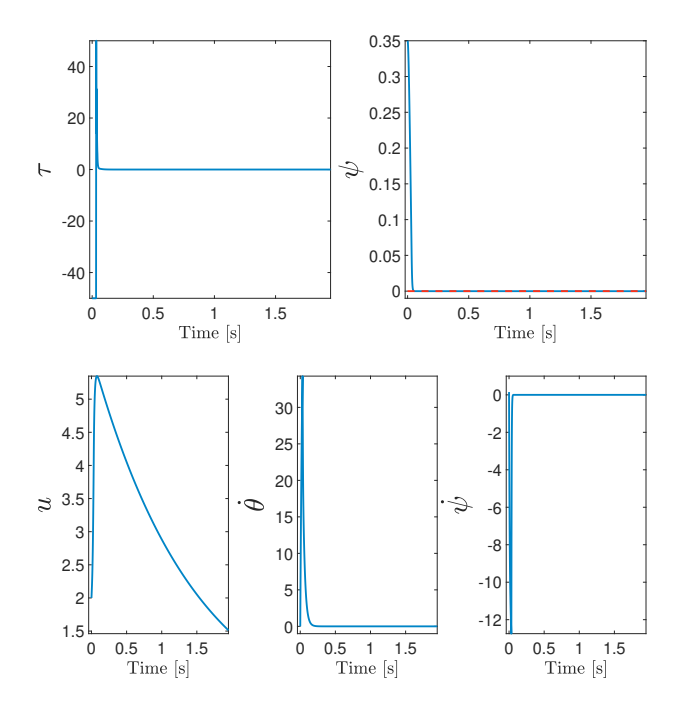


Fig. 3. Koopman MPC with no disturbance in the system. Using weights $q_{\psi}=10$ and $r=10^{-7}$

We also test our Koopman MPC with random disturbance $(|d| \leq 10^{-3})$ in the system among the four states with similar perturbed initial conditions as shown in Fig.(4). The MPC with the weights $q_{\psi} = 10$, $r = 10^{-7}$ stabilizes the system with initial periodic torque to bring the roll angle to zero and then counters the disturbance to keep the roll angle at zero reference.

5. CONCLUSION

The model of the dynamics of a Chaplygin sleigh with additional roll dynamics is a useful starting point for fishlike aquatic robots and personal transportation systems. It is also a useful addition to the class of problems related to the stabilization of an inverted pendulum. We framed the problem of stabilizing the pendulum on an underactuated nonholonomic system as an optimal control problem by first considering a linear representation of the dynamics in a lifted space via the Koopman operator. Monomials of upto degree 4 in the reduced velocities formed the bases for the lifted space. In this high dimensional linear setting, the resulting constraints are linear in the lifted states. This linear optimal control problem is solved using MPC resulting in a torque (the control) that stabilizes the roll angle of the Chaplygin sleigh. We showed through numerical simulations that stabilization was possible with and without disturbances in the roll angular velocity.

The approach in this paper has the advantage of being systematically generalized for stabilization of equilibria of systems with increased model complexity due to additional degrees of freedom, additional nonholonomic constraints, hydrodynamic effects in the case of aquatic robots, model uncertainty and actuator saturation. It can also be generalized to problems of path tracking.

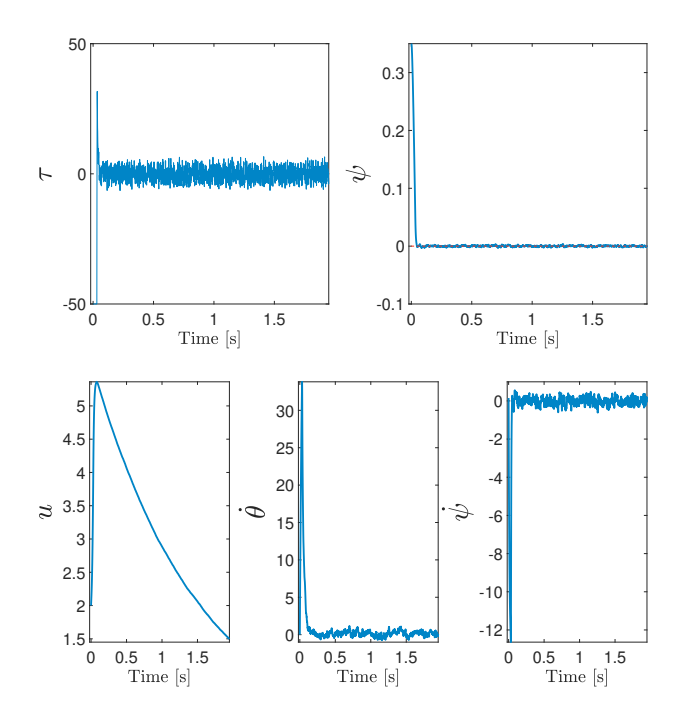


Fig. 4. Koopman MPC results with the weights $q_{\psi}=10$ and $r=10^{-7}$ with random disturbance among the states

REFERENCES

Abraham, I., Torre, G.D.L., and Murphey, T.D. (2017). Model-based control using koopman operators. *Robotics*.

Bloch, A.M. (2003). Nonholonomic Mechanics and Control. Springer Verlag.

Bloch, A.M., Leonard, N.E., and Marsden, J.E. (1997). Stabilization of mechanical systems using controlled lagrangians. In *Proceedings of the Control and Decision Conference*.

Borisov, A.V. and Mamaev, I.S. (2003). On the history of the development of the nonholonomic mechanics. *Regular and Chaotic Dynamics*, 7(1), 43–47.

Borisov, A.V., Mamaev, I.S., and Ramodanov, S.M. (2007). Dynamic interaction of point vortices and a twodimensional cylinder. *Journal of Mathematical Physics*.

Budisic, M., Mohr, R., and Mezić, I. (2012). Applied koopmanism. Chaos: An Interdisciplinary Journal of Nonlinear Science, 22, 047510.

De Luca, A., Oriolo, G., and Vendittelli, M. (2000). Stabilization of the unicycle via dynamic feedback linearization. *IFAC Proceedings Volumes*, 33(27), 687–692. 6th IFAC Symposium on Robot Control (SYROCO 2000), Vienna, Austria, 21-23 September 2000.

Free, B.A., Lee, J., and Paley, D.A. (2020). Bioinspired pursuit with a swimming robot using feedback control of an internal rotor. *Bioinspiration and Biomimetics*, 15(3), 035005.

Korda, M. and Mezic, I. (2018). Linear predictors for nonlinear dynamical systems: Koopman operator meets model predictive control. *Automatica*, 149–160.

Lasota, A. and Mackey, M.C. (1994). Chaos, Fractals, and Noise: Stochastic Aspects of Dynamics. Springer.

Ma, X., Huang, B., and Vaidya, U. (2019). Optimal quadratic regulation of nonlinear system using koopman

operator. In Proceedings of the American Control Conference, 4911–4916. IEEE.

Neimark, J.I. and Fufaev, N.A. (1972). Dynamics of Nonholonomic systems. AMS.

Otto, S.E. and Rowley, C.W. (2021). Koopman operators for estimation and control of dynamical systems. *Annual* Review of Control, Robotics, and Autonomous Systems, 4, 59–87.

Pollard, B. and Tallapragada, P. (2017). An aquatic robot propelled by an internal rotor. *IEEE/ASME Transaction on Mechatronics*, 22(2), 931–939.

Tallapragada, P. (2015). A swimming robot with an internal rotor as a nonholonomic system. *Proceedings* of the American Control Conference, 2015.

Tallapragada, P. and Kelly, S.D. (2016). Integrability of velocity constraints modeling vortex shedding in ideal fluids. *Journal of Computational and Nonlinear Dynamics*, 12(2), 021008.

Thomas, M., Bandyopadhyay, B., and Vachhani, L. (2019). Finite-time posture stabilization of the unicycle mobile robot using only position information: A discrete-time sliding mode approach. *International Journal of Robotics Research*, 29(6), 1990–2006.

Webb, P.W. and Weihs, D. (2015). Stability versus maneuvering: Challenges for stability during swimming by fishes. *Integrative and Comparative Biology*, 55(4), 753–764.

Williams, M.O., Kevrekidis, I.G., and Rowley, C.W. (2015). A data-driven approximation of the koopman operator: Extending dynamic mode decomposition. Journal of Nonlinear Science, 25(6), 1307–1346.

Y. Han, W.H. and Vaidya, U. (2020). Deep learning of koopman representation for control. In *Proceedings of* the Control and Decision Conference, 1890–1895. IEEE.

Zenkov, D.V., Bloch, A.M., and Marsden, J.E. (1999). Stabilization of the unicycle with rider. In *Proceedings* of the Control and Decision Conference.

Zenkov, D.V., Bloch, A.M., and Marsden, J.E. (2002). The lyapunov–malkin theorem and stabilization of the unicycle with rider. *Systems Control Letters*, 45(4), 293–302.